PNAS Nexus, 2024, 3, 1–14
https://doi.org/10.1093/pnasnexus/pgae053
Advance access publication 6 February 2024
Research Report

Independent metabolism of oligosaccharides is the keystone of synchronous utilization of cellulose and hemicellulose in *Myceliophthora*

Jia Liu[a,b,1], Meixin Chen[a,b,1], Shuying Gu[a,b], Rui Fan[a,b], Zhen Zhao[a,b], Wenliang Sun[a,b], Yonghong Yao[a,b], Jingen Li[a,b,*] and Chaoguang Tian[a,b,*]

[a]Key Laboratory of Engineering Biology for Low-carbon Manufacturing, Tianjin Institute of Industrial Biotechnology, Chinese Academy of Sciences, Tianjin 300308, China
[b]National Technology Innovation Center of Synthetic Biology, Tianjin 300308, China
*To whom correspondence should be addressed: Email: li_jg@tib.cas.cn (J.Li); Email: tian_cg@tib.cas.cn (C.T.)
[1]J.Liu and M.C. contributed equally to this work.
Edited By: Li-Jun Ma

Abstract

The effective utilization of cellulose and hemicellulose, the main components of plant biomass, is a key technical obstacle that needs to be overcome for the economic viability of lignocellulosic biorefineries. Here, we firstly demonstrated that the thermophilic cellulolytic fungus *Myceliophthora thermophila* can simultaneously utilize cellulose and hemicellulose, as evidenced by the independent uptake and intracellular metabolism of cellodextrin and xylodextrin. When plant biomass serviced as carbon source, we detected the cellodextrin and xylodextrin both in cells and in the culture medium, as well as high enzyme activities related to extracellular oligosaccharide formation and intracellular oligosaccharide hydrolysis. Sugar consumption assay revealed that in contrast to inhibitory effect of glucose on xylose and cellodextrin/xylodextrin consumption in mixed-carbon media, cellodextrin and xylodextrin were synchronously utilized in this fungus. Transcriptomic analysis also indicated simultaneous induction of the genes involved in cellodextrin and xylodextrin metabolic pathway, suggesting carbon catabolite repression (CCR) is triggered by extracellular glucose and can be eliminated by the intracellular hydrolysis and metabolism of oligosaccharides. The xylodextrin transporter MtCDT-2 was observed to preferentially transport xylobiose and tolerate high cellobiose concentrations, which helps to bypass the inhibition of xylobiose uptake. Furthermore, the expression of cellulase and hemicellulase genes was independently induced by their corresponding inducers, which enabled this strain to synchronously utilize cellulose and hemicellulose. Taken together, the data presented herein will further elucidate the degradation of plant biomass by fungi, with implications for the development of consolidated bioprocessing-based lignocellulosic biorefinery.

Keywords: *Myceliophthora thermophila*, cellulose and hemicellulose, independent utilization, carbon catabolite repression, fungal biotechnology

Significance Statement

Efficient utilization of plant biomass is critical for the cost-effective production of biofuels and biochemicals. We demonstrate the synchronous utilization of cellulose and hemicellulose in *Myceliophthora thermophila*. Systems biology and genetic studies revealed that carbon catabolite repression (CCR) is triggered by extracellular glucose. This fungus bypasses CCR effect by decomposing cellulose and hemicellulose smartly into oligosaccharides, which are then absorbed into cells for further hydrolysis and metabolism. This enables efficient utilization of both cellulose and hemicellulose. Independent induction of cellulolytic and hemicellulolytic enzymes further promote degradation of plant biomass. Additionally, xylodextrin transporter MtCDT-2 has high tolerance to cellobiose, which facilitates the efficient uptake of xylodextrin. These findings present a strategy for efficient utilization of plant biomass in future biorefineries.

Introduction

Plant biomass is the most abundant renewable resource on earth and considered as a potential feedstock for producing biofuels and biochemicals. Lignocellulosic biomass is primarily composed of cellulose, hemicellulose, and lignin, combining to form a complex rigid structure that is difficult to degrade (1). The efficient and complete utilization of all components of plant biomass is critical to the economic viability of lignocellulosic biorefineries.

Competing Interest: The authors declare no competing interest.
Received: April 25, 2023. **Accepted:** January 29, 2024

Cellulose is a homopolymer composed exclusively of hexose sugars. It consists of linear chains of D-glucopyranose units, each linked by β-1,4-glycosidic bonds. These chains are further stabilized by both intramolecular and intermolecular hydrogen bonds (2). Hemicellulose, which is interwoven with cellulose fibers, is a diverse biopolymer. Its composition includes xylose, arabinose, mannose, galactose, among other sugars, contributing to its heterogeneity (3). Xylan, a predominant form of hemicellulose in plant cell walls, features a linear backbone of β-1,4-linked xylosyl residues. This structure is occasionally modified by the addition of side groups, such as arabinose and glucuronic acid, which can influence its properties and interactions (4). In traditional biorefineries, fermentable sugars are obtained from biomass via a pretreatment and saccharification, with glucose and xylose being the most abundant monosaccharides in the hydrolysate (5). The asynchronous and inefficient utilization of monosaccharides due to carbon catabolite repression (CCR) in the microorganisms used for fermentation is a major factor preventing the cost-effective bioconversion of plant biomass (6–8). Furthermore, some microorganisms traditionally used for fermentations (e.g. *Saccharomyces cerevisiae*) lack pathways for the catabolism of xylose and arabinose, which are the main building blocks of hemicellulose. To overcome these problems, rational pathway engineering (9, 10), evolutionary engineering (11, 12), and global regulatory system rewiring (13, 14) have been applied for increasing the efficiency of xylose assimilation. Moreover, the engineering of sugar transporter (15, 16) and adjustments to the metabolic flux of glucose and xylose (17, 18) have been performed to enable the simultaneous utilization of glucose and xylose. Nevertheless, the catabolic rate of xylose is still significantly slower than that of glucose. In addition, the cofermentation of cellobiose and xylose has been proposed as an alternative strategy, as replacing glucose with cellobiose eliminates the inhibitory effects of glucose on xylose uptake by *S. cerevisiae* (19).

Compared with the process of separate hydrolysis and fermentation with abundant monosaccharides as intermediate products, consolidated bioprocessing (CBP) that integrates enzyme production, saccharification, and fermentation in one step by one or more microorganisms offers a viable alternative for the efficient degradation and utilization of cellulose and hemicellulose (20). Several filamentous fungi have evolved sophisticated enzymatic machineries to directly deconstruct biomass into soluble fermentable sugars (21–23), making them potentially useful for CBP. The synthesis and secretion of these lignocellulolytic enzymes are tightly regulated in different nutrient environments, in which cellulase and hemicellulase can be induced by their respective substrates (i.e. cellulose and hemicellulose, respectively) to initiate the carbon utilization (24–26). Unlike the single carbon source, lignocellulosic biomass has a complex composition that requires filamentous fungi to precisely regulate carbon metabolism-related processes during biomass degradation. However, it remains unclear how filamentous fungi coordinate the metabolism of different lignocellulose components, especially cellulose and hemicellulose, in the face of a complex lignocellulose. Earlier research confirmed that CCR is an evolved trait in filamentous fungi (8), and that it affects the production of cellulolytic enzymes as well as the uptake and catabolism of other carbon sources in the presence of glucose (27–29). The strategies employed by filamentous fungi to mitigate CCR and maintain effective lignocellulosic degradation need to be elucidated.

Myceliophthora thermophila, which can efficiently degrade biomass (30), has presented a prospect in the development of cell factories to produce fuels and chemicals directly from lignocellulose by CBP (31). In the previous study, we found that *M. thermophila* could efficiently produce malic acid directly from corncobs, with no detectable accumulation of pentose and hemicellulose during the fermentation process. This is inconsistent with the belief that pentose metabolism is inhibited by glucose during biomass hydrolysis, suggestive of the synchronous utilization of cellulose and hemicellulose in *M. thermophila*. The current investigation was conducted to further explore this interesting phenomenon. We revealed that in this thermophilic fungus, CCR due to extracellular glucose can be largely avoided by using cellodextrin and xylodextrin derived from the degradation of cellulose and hemicellulose via the independent induction of cellulolytic and hemicellulolytic enzymes. Cellodextrin and xylodextrin are defined as β-1,4-D-glucosyl- and xylosyl-oligosaccharides, respectively, with a polymerization degree between 2 and 7 (32, 33). The xylodextrin transporter MtCDT-2, which can tolerate high cellobiose concentrations, facilitates the synchronous utilization of cellodextrin and xylodextrin. These findings will be beneficial to clarifying the metabolic landscape of the filamentous fungi used for degrading lignocellulose as well as for improving the selection of chassis cells for CBP and engineering various cell factories to produce natural compounds.

Results

Synchronous utilization of cellulose and hemicellulose in *M. thermophila*

To clarify the utilization of cellulose and hemicellulose from plant biomass by *M. thermophila*, the fungus was cultured using raw corncob as the carbon source and the residual polysaccharides were assayed. Cellulose and hemicellulose were coutilized by *M. thermophila* (Fig. 1A), with no obvious CCR. The assay of sugar fragments revealed the presence of large quantities of oligosaccharides, primarily cellobiose (G2), xylobiose (X2), and xylotriose (X3), as well as monosaccharides, including glucose (G1) and xylose (X1), in the culture supernatant of *M. thermophila* grown on corncobs (Figs. 1C and S1A). These results were consistent with those for the *M. thermophila* grown in medium containing 1% Avicel and 1% xylan (AX) (Figs. 1D and S1B), which was used to mimic the degradation of plant biomass. Considering the consumption of xylose, cellobiose, and xylobiose was strongly inhibited in the presence of glucose (Figs. 1B and S2), we hypothesized that cellodextrin/xylodextrin enter cells prior to hydrolysis and catabolism. To test this hypothesis, the main extracellular disaccharides, cellobiose and xylobiose, were used as carbon sources to examine sugar consumption. Surprisingly, the experiment of sugar consumption revealed cellobiose and xylobiose were efficiently and simultaneously utilized (Fig. 1E). Additionally, trace amounts of monosaccharides were detected in the medium during the disaccharide consumption test. Consistent with this synchronous utilization pattern, the total sugar consumption efficiency was much higher for the mixed sugar of cellobiose and xylobiose (G2X2) than for cellobiose or xylobiose (Fig. 1F). The examination of polysaccharide hydrolysis and the synchronous consumption of cellodextrin and xylodextrin suggested oligosaccharides might be important mediators of the efficient simultaneous utilization of cellulose and hemicellulose in *M. thermophila*.

According to these results, we speculated that extracellular hydrolytic enzymes are prone to degrade cellulose and hemicellulose to produce oligosaccharides. To quantify the hydrolytic capacity during biomass utilization, the activities of extracellular

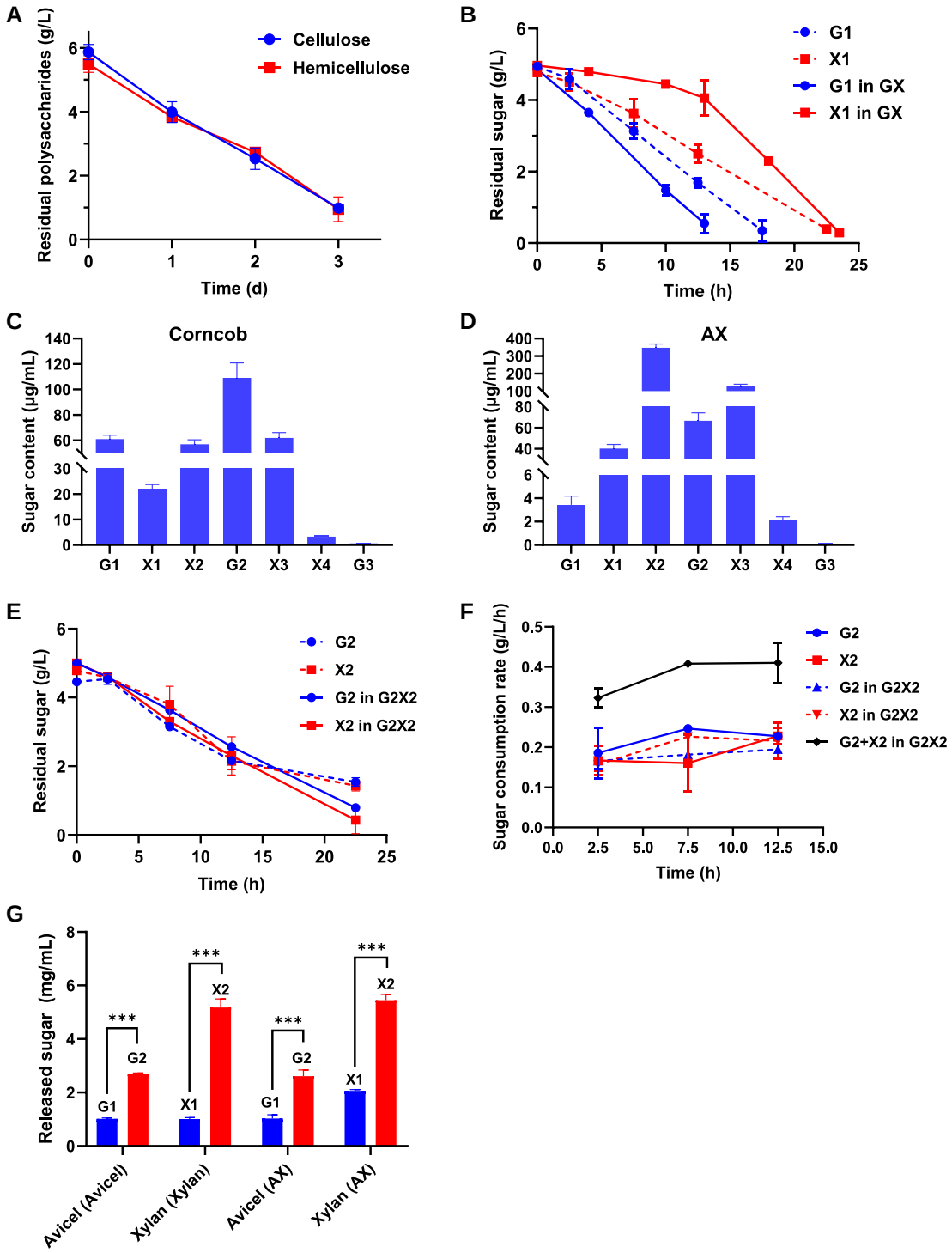

Fig. 1. Synchronous utilization of cellulose and hemicellulose in *M. thermophila*. A) Utilization of cellulose and hemicellulose by *M. thermophila* during cultivation on 2% corncob substrate. B) Residual sugar content in the medium when *M. thermophila* was cultured using G1 (0.5% glucose), X1 (0.5% xylose), or GX (0.5% glucose and 0.5% xylose) as the carbon sources. C) and D) Analysis of extracellular oligosaccharide content detected by HPAEC-PAD chromatograms in *M. thermophila* cultures using 2% corncob and AX (1% Avicel and 1% xylan) as the carbon sources, respectively. E) Residual sugar content in the medium when *M. thermophila* was cultured using 0.5% cellobiose (G2), 0.5% xylobiose (X2), or G2X2 (0.5% cellobiose and 0.5% xylobiose) as the carbon sources. F) The consumption rate of sugar when *M. thermophila* was cultured on G2, X2, or G2X2. G) Hydrolytic activity of *M. thermophila* culture filtrates. Culture and induction conditions are detailed in the Materials and methods section. For assays, treated culture filtrates (50 μg protein) were added to either 2% Avicel or 2% xylan, followed by incubation at 45 °C for 24 h. Subsequent analysis focused on monosaccharides and disaccharides, specifically targeting glucose and cellobiose for 2% Avicel, and xylose and xylobiose for 2% xylan. The values and error bars represent means and SD of independent triplicate experiments, respectively. *** represents significant difference at $P < 0.001$. ns, no statistical significance; plas, plasma membrane-bound; cyto, cytoplasm; extr, extracellular; G1, glucose; G2, cellobiose; G3, cellotriose; X1, xylose; X2, xylobiose; X3, xylotriose; X4, xylotetraose.

enzymes induced by Avicel, xylan, and AX were assayed with Avicel or xylan used as the substrate. Both cellulases and hemicellulases were induced on AX medium; these enzymes catalyzed the production of more disaccharides (cellobiose and xylobiose) than monosaccharides (glucose and xylose) (Fig. 1G). Similar activities were detected when samples were induced on Avicel and xylan media (Fig. 1G). These results reflected a substantial increase in the activities of lignocellulolytic enzymes that convert cellulose and hemicellulose to oligosaccharides during plant biomass degradation.

The universality of the synchronous utilization of cellobiose and xylobiose among cellulolytic fungi was assessed by analyzing the sugar consumption of *Neurospora crassa* and *Trichoderma reesei*. Unlike *M. thermophila*, these two fungi differentially utilized cellobiose and xylobiose. For both *N. crassa* and *T. reesei*, the cellobiose consumption rate was higher than the xylobiose consumption rate. Moreover, when the fungi were grown on G2X2, the attenuated metabolism of sugars was more obvious for xylobiose than for cellobiose (Fig. S3A and C). Furthermore, the total sugar consumption of *N. crassa* and *T. reesei* in the G2X2 medium was similar to that in the cellobiose culture (Fig. S3B and D) and the presence of cellobiose appeared to suppress the utilization of xylobiose (Fig. S3A and C).

Intracellular β-glucosidase and β-xylosidase activities play a dominant role in the hydrolysis of oligosaccharides

During the process of biomass utilization, a variety of carbohydrate-active enzymes are secreted into the extracellular environment to break down cellulose and hemicellulose into their respective oligosaccharides, which are subsequently hydrolyzed by β-glucosidase (BGL) and β-xylosidase (BXL), either inside or outside of the cell, to liberate the constituent monosaccharides (34, 35). Considering the observations that the low extracellular monosaccharide content and the synchronous consumption of cellobiose and xylobiose in the G2X2 medium, we speculated that *M. thermophila* have reduced the formation of extracellular monosaccharides by cleaving oligosaccharides intracellularly. To verify this hypothesis, the intracellular sugar metabolites, when corncob and AX were used as substrates, were analyzed. As expected, both cellodextrin and xylodextrin were detected within cells (Figs. 2A and S4).

The hydrolysis of cellodextrin/xylodextrin into monosaccharides requires high BGL/BXL activities. To determine where oligosaccharide hydrolysis mainly occurs, the extracellular/intracellular BGL and BXL activities of *M. thermophila* were examined under different polysaccharide conditions. The intracellular BGL/BXL activities were much higher than the extracellular enzyme activities (per unit culture volume) in response to Avicel, xylan, or AX (Fig. 2B). Because the fungal mycelium was relatively small, the intracellular enzymes (BGL/BXL) clearly outperformed the extracellular enzymes in terms of activity per unit volume (Figs. 1G and 2B), facilitating the intracellular hydrolysis of oligosaccharides.

Uptake and intracellular hydrolysis of cellodextrin and xylodextrin derived from plant biomass

To further investigate the intracellular degradation and metabolism of oligosaccharides in *M. thermophila*, a comparative analysis of transcriptomic data was performed following the induction in the starvation medium (no carbon source, NC) or in the media supplemented with Avicel, xylan, or AX. Consistent with the results of previous study that showed intracellular BGLs are the main enzymes responsible for cellobiose degradation (35), three genes encoding intracellular BGLs (Mycth_115968, Mycth_62925, and Mycth_2302509) were more highly expressed in samples grown in medium containing Avicel than those in samples under starvation condition, whereas the opposite pattern was observed for two genes, encoding extracellular BGLs (Mycth_2059579 and Mycth_80304) (Fig. 3A and Dataset S3). In response to xylan, the expression levels of Mycth_39555 (*bxl1*), Mycth_80104 (*bxl2*), and Mycth_104628, which encode intracellular BXLs, and Mycth_2301869 (*bxl3*), encoding an extracellular BXL, were upregulated, compared with these under NC condition (Fig. 3A and Dataset S3).

To evaluate the role of BXLs during xylodextrin assimilation, two highly induced intracellular BXL genes (*bxl1* and *bxl2*) and one extracellular BXL gene (*bxl3*) were deleted. Specifically, five mutants were generated, including three single-gene mutants (Δ*bxl1*, Δ*bxl2*, and Δ*bxl3*), a double-gene mutant (Δ*bxl1*Δ*bxl2*), and a triple-gene mutant (Δ*bxl1*Δ*bxl2*Δ*bxl3*). The BXL activity assay indicated that the deletion of *bxl1* resulted in an almost complete lack of intracellular BXL activity (Fig. 3B). Similarly, the deletion of *bxl2* also resulted in a significant decrease in intracellular BXL activity (Fig. 3B). However, the deletion of *bxl3* had no effect on intracellular BXL activity (Fig. 3B). In contrast, increased extracellular BXL activity was detected for the Δ*bxl1*, Δ*bxl2*, and Δ*bxl1*Δ*bxl2* mutants, but the deletion of *bxl3* did not significantly affect extracellular BXL activity (Fig. 3C). These findings suggest that BXL1 and BXL2 are mainly responsible for the β-1,4-xylosidase activity in *M. thermophila*.

To confirm that intracellular BXLs might be the primary enzymes mediating xylodextrin hydrolysis during plant biomass degradation, the wild-type (WT) and Δ*bxl1*Δ*bxl2* strains grown on xylan were compared in terms of growth phenotypes and intracellular sugar fractions. Compared with the WT, the xylodextrin content (especially cellobiose) increased significantly in Δ*bxl1*Δ*bxl2*, but xylose accumulation decreased (Fig. 3D). The enhanced accumulation of intracellular oligosaccharides and the decrease in the monosaccharide content reflect the importance of BXL1/2 for the hydrolysis of intracellular oligosaccharides. There was also a marked decrease in the growth of the Δ*bxl1*Δ*bxl2* mutant. More specifically, the Δ*bxl1*Δ*bxl2* biomass was only 28.18% of the WT biomass on xylan (Fig. 3E). Furthermore, the double mutation in Δ*bxl1*Δ*bxl2* resulted in a severe decrease in xylobiose utilization (Fig. 3F). These results imply that intracellular BXLs are essential for xylodextrin degradation.

The transport of monosaccharides/oligosaccharides into cells, which is a prerequisite for sugar metabolism, is dependent on transporters. The transcriptomic analysis indicated that the expression of a putative sugar transporter gene (Mycth_114107, *Mtcdt-2*) was highly induced on Avicel, xylan, and AX, compared with these under starvation condition (Fig. 3A and Dataset S3), suggesting it may contribute to oligosaccharide or monosaccharide transport. Protein encoded by *Mtcdt-2* exhibited a high identity (75.91%) with the cellodextrin and xylodextrin transporter NcCDT-2 in *N. crassa* (36, 37). Consequently, mutant Δ*Mtcdt-2* was constructed to determine whether *Mtcdt-2* contributes to oligosaccharide transport. When cultured on xylan, Δ*Mtcdt-2* had a severe growth defect, but its growth was not significantly altered when cultured on Avicel (Fig. 3E), suggesting that MtCDT-2 plays an important role in xylan utilization. In addition, the xylodextrin and xylose contents were much lower in Δ*Mtcdt-2* than in the WT when grown on xylan (Fig. 3D). To further clarify the effect

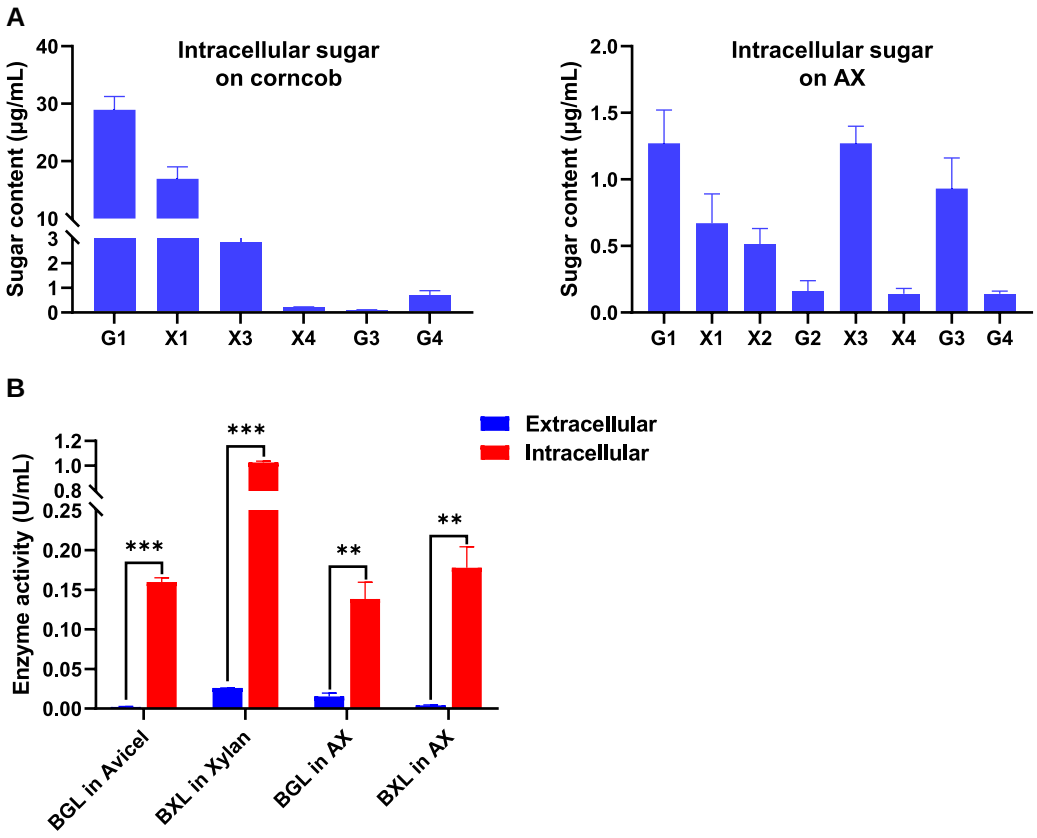

Fig. 2. The intracellular activities of BGL and BXL play a dominant role in the hydrolysis of oligosaccharides. A) Intracellular oligosaccharide content detected by HPAEC-PAD chromatogram in *M. thermophila* cultured with 2% corncob or AX (1% Avicel and 1% xylan). B) Extracellular and intracellular activities of BGL and BXL in *M. thermophila* cultured with 2% Avicel, 2% xylan, or AX (1% Avicel and 1% xylan) as the carbon sources. The values and error bars represent means and SD of independent triplicate experiments, respectively. ns, no statistical significance. ** and *** represent significant difference at $P < 0.01$ and $P < 0.001$, respectively.

of MtCDT-2 on xylodextrin assimilation, the sugar consumption of Δ*Mtcdt-2* was examined using the media containing xylose or xylobiose. The xylose consumption rate of the Δ*Mtcdt-2* mutant was similar to that of the WT, implying xylose transport was normal in Δ*Mtcdt-2* (Fig. S7A). However, the deletion of *Mtcdt-2* adversely affected xylobiose consumption (Fig. 3F). Meanwhile, xylose was undetectable in the supernatant during xylobiose utilization (Fig. S7B). The growth defect was also observed in the medium supplemented with xylotriose (Fig. S7C). These results confirm the importance of xylodextrin transport into cells for xylan utilization. The deletion of *Mtcdt-2* inhibited the sugar consumption of the mutant on medium supplemented with G2X2 (Fig. S8), further implying MtCDT-2 is crucial for the synchronous utilization of oligosaccharides (also AX) in *M. thermophila*.

The findings indicate BXL1, BXL2, and MtCDT-2 directly affect intracellular oligosaccharide utilization. Moreover, the deletion of the corresponding genes significantly promoted protein secretion and endo-xylanase (XLN) activity (Fig. 3G), suggesting that xylodextrin is closely related to the induction of hemicellulases, which is similar to the enhanced cellulase activity in *N. crassa* on Avicel resulting from the deletion of BGLs (23). Furthermore, the deletion of *Mtcdt-2* led to a significant decrease in intracellular BXL activity, but increased extracellular BXL activity (Fig. 3B and C), thereby restricting extracellular xylodextrin accumulation.

Intracellular hydrolysis and metabolism of cellodextrin and xylodextrin eliminated the CCR in *M. thermophila*

When *M. thermophila* was grown in media containing mixed-carbon sources, glucose inhibited monosaccharide/oligosaccharide metabolism. In the presence of glucose, cellobiose was consumed much less efficiently, while xylobiose was barely utilized until glucose was depleted (Fig. S2). The transcriptome data showed that genes associated with intracellular xylodextrin hydrolysis and the xylose catabolic pathway exhibited significantly down-regulated expression levels on mixed glucose–xylose (GX) and mixed glucose–xylobiose (GX2), compared to these on G2X2 and xylobiose (Fig. 4A, B and Dataset S4). Moreover, the expression of these genes in *M. thermophila* was much lower on GX2 than on GX (Fig. 4A and Dataset S4), indicative of the relatively severe glucose-related CCR effect on xylobiose utilization.

In contrast to the inhibitory effects of glucose on xylose and oligosaccharide metabolism, the pathway mediating the intracellular hydrolysis of oligosaccharides enabled the synchronous utilization of cellobiose and xylobiose (Fig. 1B, E, and F). Even though glucose and xylose were produced intracellularly (Figs. 2A and S4), there appeared to be no associated CCR effect. To characterize the CCR effect, the expression levels of the genes involved in intracellular oligosaccharide metabolism were analyzed under different carbon conditions. The expression of the major intracellular oligosaccharide hydrolysis genes (*bxl1* and *bxl2*) increased substantially

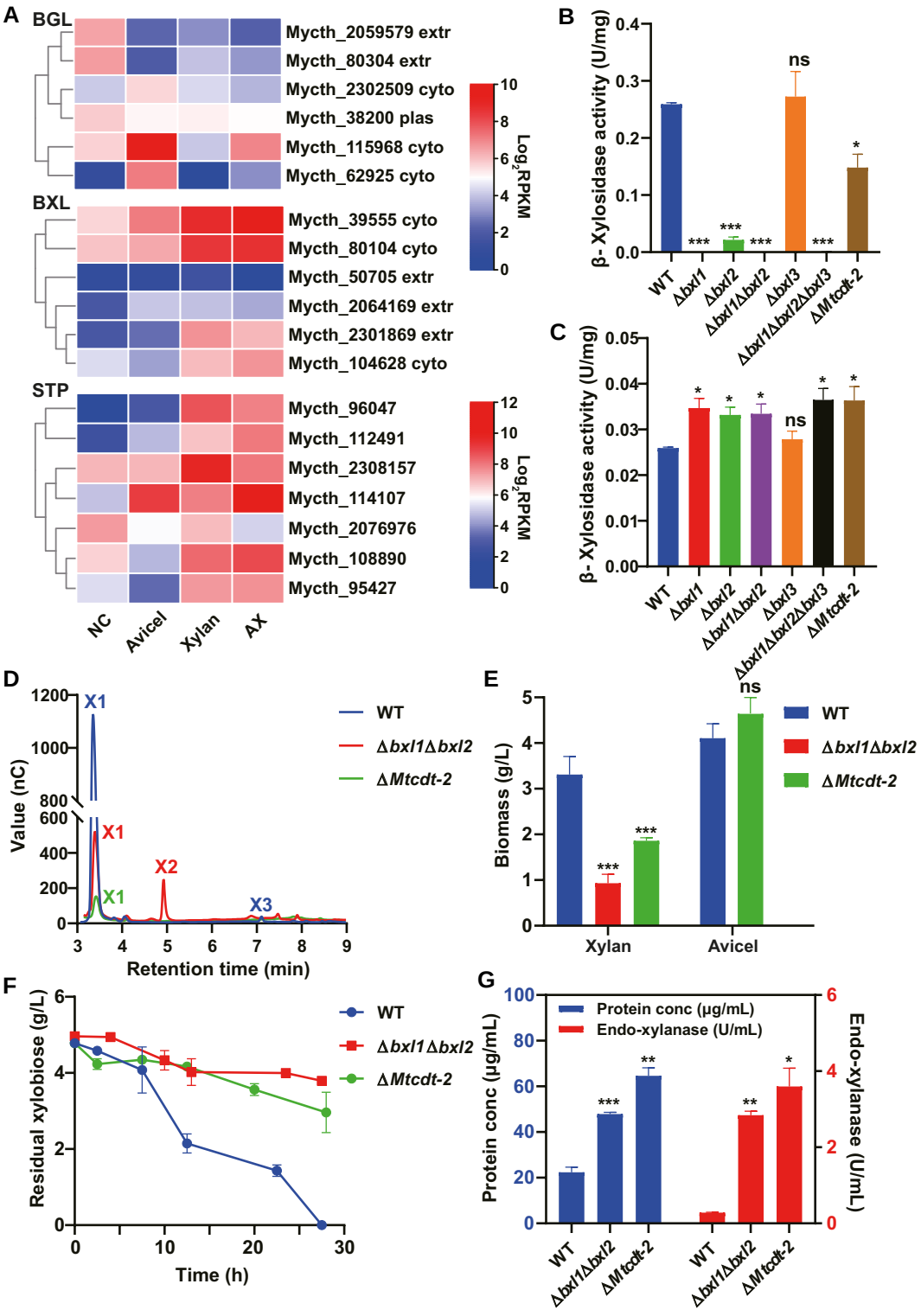

Fig. 3. Uptake and intracellular hydrolysis of cellodextrin and xylodextrin derived from plant biomass. A) Hierarchical cluster analysis of the expression of BGL, BXL, and sugar transporter (STP) genes in *M. thermophila* after the 4 h induction with no carbon (NC), Avicel, xylan, or AX (Avicel and xylan). Intracellular B) and extracellular C) BXL activity in the *M. thermophila* wild-type (WT) strain and its mutant strains following 1 day of incubation in 2% xylan medium. D) Intracellular monosaccharide and oligosaccharide contents in WT, Δ*bxl1*Δ*bxl2*, and Δ*Mtcdt-2* strains grown on xylan for 2 days. E) Dry cell weight of the WT, Δ*bxl1*Δ*bxl2*, and Δ*Mtcdt-2* strains grown on xylan for 1 day and on Avicel for 3 days. F) Xylobiose consumption of the WT, Δ*bxl1*Δ*bxl2*, and Δ*Mtcdt-2* strains. G) Protein concentration and endo-xylanase activity in the supernatant of the WT, Δ*bxl1*Δ*bxl2*, and Δ*Mtcdt-2* strains after the 2 days culture on xylan. plas, plasma membrane-bound; cyto, cytoplasm; extr, extracellular. The values and error bars represent means and SD of independent triplicate experiments, respectively. ns, no statistical significance. *, **, and *** represent significant difference at $P < 0.05$, $P < 0.01$, and $P < 0.001$, respectively.

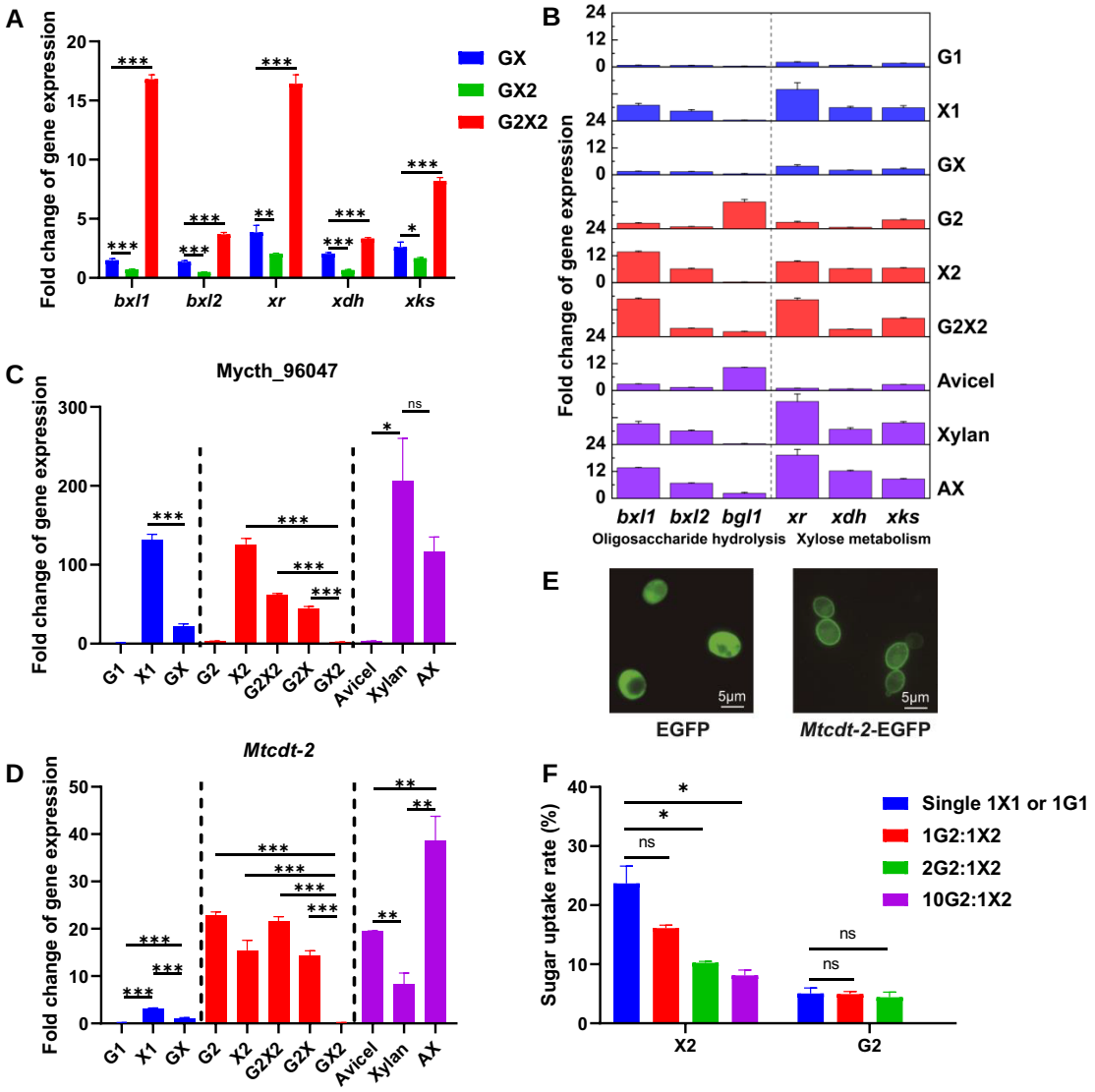

Fig. 4. Intracellular hydrolysis and metabolism of cellodextrin and xylodextrin eliminates carbon catabolite repression. A) The relative expression levels of *bxl1*, *bxl2*, *xr*, *xdh*, and *xks* in *M. thermophila* on GX (glucose and xylose), GX2 (glucose and xylobiose), or G2X2 (cellobiose and xylobiose), compared with those under no carbon condition. B) The relative expression levels of oligosaccharide hydrolase and xylose catabolism genes on different carbon sources, compared to those under starvation condition. The relative expression levels of Mycth_96047 C) and *Mtcdt-2* D) in *M. thermophila* grown on G1 (glucose), X1 (xylose), GX, G2 (cellobiose), X2 (xylobiose), G2X2, G2X (cellobiose and xylose), GX2, Avicel, xylan, and AX, compared to the starvation condition. E) Confocal fluorescence microscopy images of *S. cerevisiae* strain EBY.VW4000 cells harboring EGFP and MtCDT-2-EGFP. F) Sugar uptake rates of xylobiose (X2) and cellobiose (G2) in the strain EBY.VW4000 with MtCDT-2, When G2, X2, or a mixed sugar composition of G2 and X2 (in ratios of 1:1, 2:1, and 10:1) were used as the substrates. The values and error bars represent means and SD of independent triplicate experiments, respectively. ns, no statistical significance. *, **, and *** represent significant difference at $P < 0.05$, $P < 0.01$, and $P < 0.001$, respectively.

under G2X2 and AX conditions, similar to the expression induced by xylobiose or xylan (Fig. 4B). The *bgl1* expression level was lower on G2X2 than on cellobiose, but it was still higher than that under starvation condition (Fig. 4B). Furthermore, the genes encoding the enzymes of xylose catabolic pathway, Mycth_43671 (xylose reductase, *xr*) and Mycth_67060 (xylulokinase, *xks*), remained high expression on G2X2 and AX, similar to these on xylobiose and xylan (Fig. 4B), whereas their expression levels were significantly lower on GX than on xylose, consistent with the suppressive effects of glucose on xylose catabolism (Figs. 4B and 1B). The derepression of the activation of genes involved in the hydrolysis and catabolism of xylobiose suggests glucose produced in the cell cannot trigger the CCR effect.

In addition to the catabolic pathway, the regulation of substrate transport and the competition for transporters may also inhibit substrate coutilization (38, 39). Although the expression of the xylose metabolic pathway genes was lower on GX than on xylose, the genes, *xr*, *xdh*, and *xks*, showed respectively 3.85-, 2.04-, and 2.61-fold higher than these under starvation condition, indicating that the xylose catabolic pathway was not completely blocked (Fig. 4B and Dataset S4). Accordingly, repressed transport may also be a factor suppressing xylose utilization. The gene ontology (GO) enrichment analysis revealed that the genes induced in xylose medium but suppressed in GX medium were enriched in the set of carbohydrate transport (Figs. 4C, D and S5, and Dataset S5). Among these transporters, the putative xylose transporter Mycth_96047, with a high identity with the xylose and glucose transporter encoded by NCU06138 in *N. crassa* (40), showed a high expression level under xylose, xylobiose, and xylan conditions, while it was strongly inhibited by glucose (Fig. 4C).

Additionally, the expression of xylodextrin transporter gene *Mtcdt-2* was also suppressed in GX medium compared to that in xylose medium (Fig. 4D). However, *Mtcdt-2* was expressed at a high level in the presence of one or more oligosaccharide/polysaccharide (Fig. 4D), which guaranteed the simultaneous utilization of cellodextrin and xylodextrin (also cellulose and hemicellulose). Previous studies showed the competition and inhibition effects of CDT-2 orthologs in transporting xylobiose and cellobiose (41). To clarify the effect of cellobiose on the ability of MtCDT-2 to transport xylobiose, codon-optimized *Mtcdt-2* was expressed in *S. cerevisiae* EBY.VW4000, and the correct membrane localization of the EGFP-tagged protein was observed using the fluorescence microscope (Fig. 4E). The activity assay of MtCDT-2 transporter indicated that the xylobiose uptake rate (23.70%) was much higher than the cellobiose uptake rate (5.04%) (Fig. 4F). In the presence of both cellobiose and xylobiose (1:1, 2:1, and 10:1), the uptake of xylobiose was greater than that of cellobiose (Fig. 4F). These results suggest that the high affinity of MtCDT-2 to xylobiose over cellobiose facilitates the rapid and sustainable uptake of xylobiose during intracellular metabolism, even in the presence of high concentrations of cellobiose.

Independently induced expression of hemicellulolytic and cellulolytic enzymes in *M. thermophila*

The coutilization of cellulose and hemicellulose depends on multiple extracellular carbohydrate-active enzymes synergistically degrading plant biomass to the corresponding oligosaccharides; these enzymes are induced by the respective substrates as well as some soluble inducers by perception pathways (26, 42).

To determine the relationships between the expression of hemicellulolytic and cellulolytic enzymes, comparative transcriptomic profiles were analyzed under starvation, cellobiose, xylobiose, and G2X2 conditions. The expression of the genes encoding hemicellulolytic enzymes and cellulolytic enzymes was highly induced by cellobiose and xylobiose, respectively, relative to these under starvation conditions (Fig. 5A and Dataset S6), suggesting the important roles of cellobiose and xylobiose in inducing corresponding cellulase and hemicellulase in *M. thermophila*. Furthermore, the expression patterns of cellulase genes on cellobiose and hemicellulase genes on xylobiose were similar to the corresponding expression patterns in *M. thermophila* on G2X2 (Fig. 5A and Dataset S6), reflecting the independently induced expression of cellulase and hemicellulase genes by cellobiose and xylobiose. Consistent with these observations, the expression levels of these cellulase genes on cellobiose and hemicellulase genes on xylobiose were most highly correlated with the corresponding expression levels in *M. thermophila* on G2X2 (Fig. 5C). Moreover, the Venn analysis showed that most of the cellulases and hemicellulases induced by cellobiose and xylobiose, including almost all of the enzymes catalyzing the hydrolysis of hemicellulose/cellulose to their constitutive oligosaccharides and monosaccharides (Fig. S6), were also induced by G2X2 (Fig. 5D and Dataset S7). This phenomenon was also revealed by the comparative analysis of the transcriptomes of the samples grown on Avicel, xylan, and AX (Fig. 5B and Dataset S6), further confirming the independent expression pattern of cellulase and hemicellulase genes in a complex biomass environment, which is essential for the efficient degradation and utilization of plant biomass.

In addition to xylobiose, the expression of hemicellulase genes was also induced by xylose (Fig. 5E and Dataset S8). However, unlike the independent induction of cellulase and hemicellulase genes by G2X2 and AX, the presence of glucose in the medium containing GX almost completely inhibited the xylose-induced expression of hemicellulase genes (Fig. 5E); a more severe inhibition was observed for the samples grown on GX2 medium (Fig. 5E). These data revealed that CCR negatively affects the induction of hemicellulase genes in *M. thermophila*. In contrast, the intracellular metabolism of G2X2 successfully bypassed the inhibition of (hemi)cellulase expression by glucose (Fig. 5E). Thus, compared with the extracellular conversion of biomass to monosaccharides, the intracellular conversion of oligosaccharides to monosaccharides circumvents the glucose-related CCR effect to enable the utilization of xylose, xylobiose, and cellobiose as well as the degradation of biomass through the independent induction of lignocellulolytic enzymes.

Discussion

Filamentous fungi possess the capacity of deconstructing lignocellulose by the synergistic action of large amounts of hydrolytic enzymes. Some soluble substrates released have been identified to induce the expression of lignocellulosic enzymes, but their functions differ among fungi. Cellobiose and its derivative can induce cellulase gene expression in *N. crassa*, *T. reesei*, and *Aspergillus* species (26, 27, 43), but not in *Phanerochaete chrysosporium* (44). Sophorose is a cellulase inducer in *T. reesei* (45, 46), but it is nonfunctional in *N. crassa* and *Aspergillus niger* (26, 47). Our transcriptome analysis indicated cellobiose can induce the expression of cellulase genes in *M. thermophila* (Fig. 5A). In *N. crassa*, the inductive effect of cellobiose is masked by its degradation to glucose by endogenous BGLs (26), while in *M. thermophila*, cellobiose can directly induce the expression of majority cellulase genes (Fig. 5A). In addition, hemicellulase gene expression is also highly induced by xylobiose and xylose (Fig. 5A and E), but xylobiose has a stronger inductive effect (Fig. 5E and Dataset S8). The deletion of *bxl1*, *bxl2*, or *Mtcdt-2* in *M. thermophila* cultured on xylan can significantly increase the extracellular xylanolytic activity (Fig. 3G), implying xylobiose or its derivatives may function as the inducer of hemicellulases, like cellobiose inducing the expression of cellulase genes.

In this study, *M. thermophila* synchronously utilized cellobiose and xylobiose (i.e. main products of lignocellulose decomposition) in the G2X2 medium (Fig. 1E and F), suggesting that cellobiose and xylobiose have two relatively independent metabolic pathways involving oligosaccharide transport, intracellular hydrolysis, and even the catabolism of their constitutive monosaccharides. Consistent with this suggestion, the xylodextrin transporter gene *Mtcdt-2*, intracellular βBXL genes *bxl1* and *bxl2*, and the xylose catabolic pathway genes were consistently highly expressed in *M. thermophila* grown in xylobiose and G2X2 media (Fig. 4B and D). In *N. crassa*, deletion of *Nccdt-2* resulted in significant growth defects on cellulose and hemicellulose (37). However, deletion of *Mtcdt-2* mainly affected the growth of mycelium on hemicellulose (xylan), indicating NcCDT-2 and MtCDT-2 differ regarding their functions related to lignocellulose utilization. Sugar transport assay using *S. cerevisiae* demonstrated the preference of MtCDT-2 to xylobiose, partly contributing to the simultaneous utilization of xylobiose and cellobiose.

The interconnections among catabolic pathways of the components from plant biomass have been investigated (39). Mannodextrins can inhibit cellulase production, thereby inhibiting the growth of *N. crassa* on cellulose. The crosstalk of perception pathways and competitive inhibition between cellodextrins and mannodextrins have been observed both during uptake by

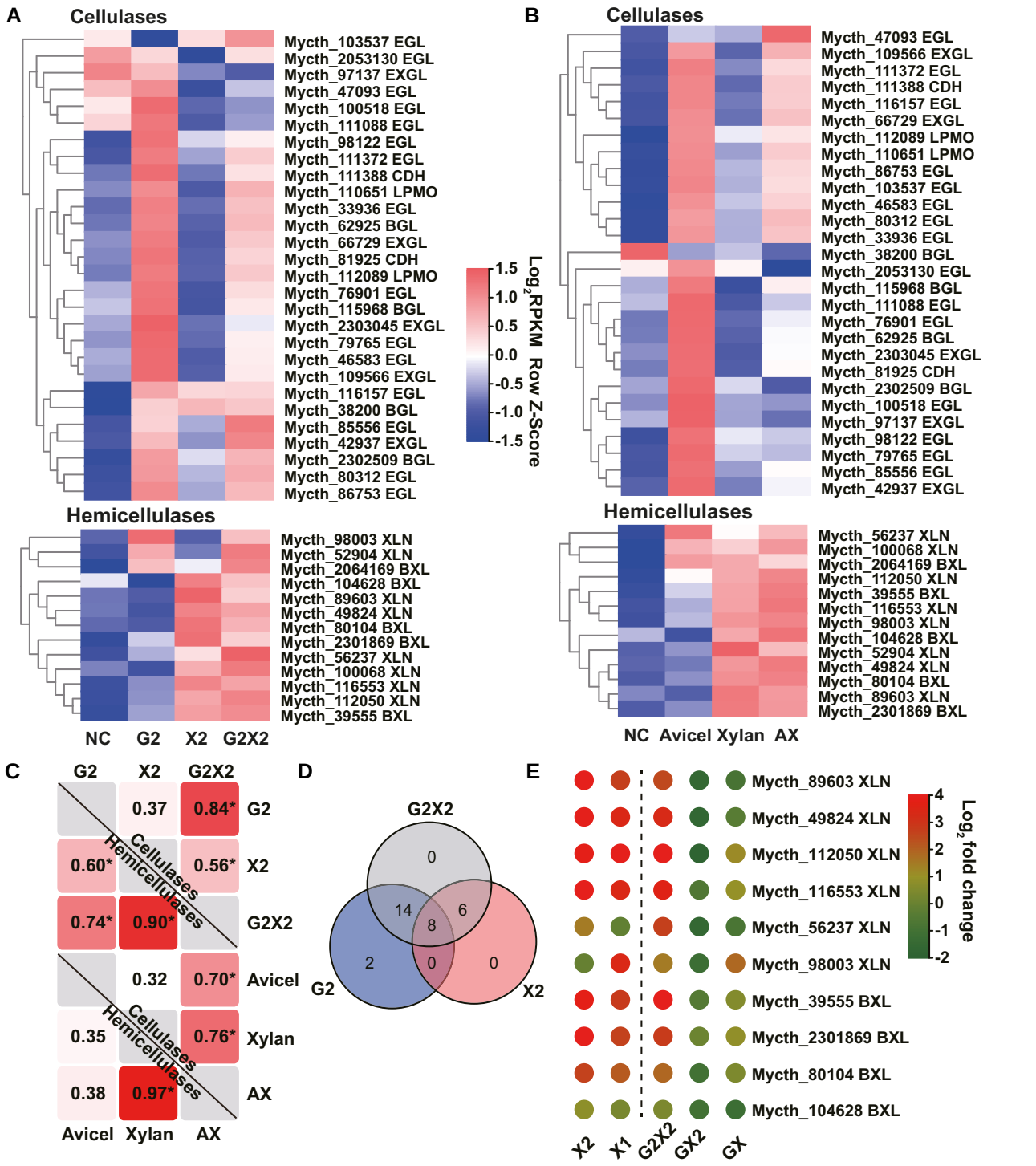

Fig. 5. Independent induction of hemicellulolytic and cellulolytic enzyme-encoding genes in *M. thermophila*. A) Hierarchical cluster analysis of the expression of cellulase and hemicellulase genes in *M. thermophila* after the 4 h induction with NC (no carbon), G2 (cellobiose), X2 (xylobiose), or G2X2 (cellobiose and xylobiose). B) Hierarchical cluster analysis of the expression of cellulase and hemicellulase in *M. thermophila* after the 4 h induction with NC, Avicel, xylan, or AX (Avicel and xylan). C) Analysis of the correlation in cellulase and hemicellulase gene expression across different carbon sources. Spearman's rank correlation test was performed to analyze correlations; $^{*}P < 0.05$. D) Venn diagram showing hemicellulase and cellulase genes with up-regulated expression in *M. thermophila* cultured on G2, X2, or G2X2, compared to the NC condition. E) Relative expression of xylan degradation-related genes under single sugar (X2 and X1) and mixed sugar (G2X2, GX2, and GX) conditions, compared to NC condition. X2, xylobiose; X1, xylose; G2X2, mixed cellobiose and xylobiose; GX2, mixed glucose and xylobiose; GX, mixed glucose and xylose. EGL, endoglucanase; EXGL, exoglucanase; CDH, cellobiose dehydrogenase; LPMO, lytic polysaccharide monooxygenase; BGL, β-glucosidase; XLN, xylanase; BXL, β-xylosidase.

cellodextrin transporters and within cells. This inhibition phenomenon was also detected in *M. thermophila* and *T. ressei*. However, the expression of cellulase and hemicellulase genes is independently induced in mixed G2X2 medium (Fig. 5A and B), indicating that the intracellular coexistence of xylodextrin/cellodextrin and their degradants (xylose and glucose) does not

trigger the crosstalk and CCR effect. Additionally, in this study, the presence of glucose inhibited the utilization of xylose, xylobiose, and cellobiose (Figs. 1B andS2). Accordingly, the CCR effect in *M. thermophila* was activated following the perception of extracellular glucose, unlike in *S. cerevisiae*, where glucose signals that activate the main glucose repression pathway are derived from the plasma membrane receptor and the intracellular intermediates of glucose catabolism (8, 48). In an earlier study on glucose and galactose utilization, the glucose concentration regulated galactose metabolism-related gene expression, which was almost completely suppressed by the treatment with 10 g/L glucose (49). In the present study, trace amounts of extracellular monosaccharides were detected during xylobiose and cellobiose metabolism (Fig. S7), suggesting that *M. thermophila* may maintain a relatively low extracellular glucose level, thereby eliminating the CCR effect during lignocellulose utilization. This may also explain why the intracellular xylobiose and cellobiose metabolism of *M. thermophila* is greater than the extracellular hydrolysis of monosaccharides. Additionally, metabolizing oligosaccharides avoids the competition for glucose with glucose-utilizing soil microbes and may be more energetically favorable because oligosaccharide transport does not consume excessive amounts of energy and enzymes do not need to be secreted (50, 51).

Intracellular oligosaccharide metabolism strategies present the advantage of *M. thermophila* in development of CBP technique, which can be borrowed for fermentation strain design. For example, a previous study involving *S. cerevisiae* confirmed the inhibition of xylose transport by glucose can be bypassed by using xylose and cellobiose as substrates (19). In terms of industrial production, the conversion of plant biomass to soluble oligosaccharides catalyzed by a hydrolytic enzyme cocktail avoids the inhibitory effects of glucose on hydrolases. Moreover, the simultaneous utilization of substrates during fermentation is ideal. Furthermore, industrial fungal strains can be rationally designed according to the cellobiose/xylobiose metabolic activities in *M. thermophila* to facilitate the simultaneous use of multiple carbon sources. In conclusion, the independent oligosaccharide catabolic pathway in the thermophilic fungus *M. thermophila* may be exploited for the simultaneous utilization of cellulose and hemicellulose in lignocellulosic biorefineries.

Materials and methods

Strains, media, and culture conditions

Myceliophthora thermophila WT strain (ATCC 42464) and its derivates were grown on 1× Vogel's minimal medium (VMM) supplemented with 2% (w/v) glucose at 35 °C for 10–15 days to obtain conidia. *Neurospora crassa* (FGSC2489) was grown on 1× VMM supplemented with 2% sucrose at 25 °C and *T. reesei* QM6a was grown on 1× VMM supplemented with 2% glucose at 30 °C to obtain conidia. Colonies were screened on media containing the appropriate antibiotics.

Saccharomyces cerevisiae EBY.VW4000 (52) was cultured in YPM medium (10 g/L yeast extract, 20 g/L peptone, and 20 g/L maltose) at 30 °C, whereas its derivatives containing the pRS426-PGK recombinant plasmid were grown on synthetic dropout (SD) medium (20 g/L maltose, 6.7 g/L YNB, and 1.92 g/L yeast synthetic dropout medium without uracil) at 30 °C.

Escherichia coli Mach1-T1 was used for the construction of recombinant plasmids. If necessary, 100 μg/mL ampicillin was added to the LB medium. The strains and plasmids used in this study are listed in Dataset S1.

Plasmid construction

Plasmids for sgRNA expression were constructed as previously described (53). Specific sgRNA target sites in *bxl1* (Mycth_39555), *bxl2* (Mycth_80104), *bxl3* (Mycth_2301869), and *Mtcdt-2* (Mycth_114107) were screened using the sgRNACas9 tool (54) with the *M. thermophila* genome sequence and the target gene as the inputs. The *M. thermophila* U6 promoter and a target-directed sgRNA fragment were amplified from the U6p-sgRNA plasmid (53), assembled by overlapping PCR, and cloned into the pJET1.2/blunt cloning vector to generate the following recombinant plasmids: U6-*bxl1*-sgRNA, U6-*bxl2*-sgRNA, U6-*bxl3*-sgRNA, and U6-*Mtcdt2*-sgRNA.

The vectors carrying donor DNA were constructed as follows. The 5′- and 3′-flanking fragments of *bxl1*, *bxl2*, *bxl3*, and *Mtcdt-2* were amplified from *M. thermophila* genomic DNA. Additionally, PtrpC-*bar* from the p0380-*bar* plasmid and PtrpC-*neo* from the p0380-*neo* plasmid were cloned using primers neo-F/R and bar-F/R, respectively. The 5′- and 3′-flanking fragments of *bxl1* and the selectable marker cassettes PtrpC-*neo* were assembled using the NEB Gibson assembly kit and cloned into between *Bgl*II and *Hin*dIII of pAN52-PtrpC-TB to generate donor DNA-*bxl1-neo*. Similarly, the 5′- and 3′-flanking fragments of *bxl2*, *bxl3*, and *Mtcdt-2* and PtrpC-*neo* were assembled to generate donor DNA-*bxl2-neo*, donor DNA-*bxl3-bar*, and donor DNA-*Mtcdt2-neo*.

To construct the recombinant plasmid for the heterologous expression of *Mtcdt-2* in *S. cerevisiae*, the genes encoding MtCDT-2, EGFP, and MtCDT-2-EGFP were amplified and separately ligated into between *Bam*HI and *Eco*RI sites of the pRS426-PGK plasmid to generate the corresponding expression vectors pRS426-PGK-EGFP, pRS426-PGK-*Mtcdt-2*, and pRS426-PGK-*Mtcdt-2*-EGFP.

The recombinant plasmids were analyzed by DNA sequencing to verify they were constructed correctly. The primers used in this study are listed in Dataset S2.

Transformation of *M. thermophila* protoplasts and *S. cerevisiae*

Transformation of *M. thermophila* protoplasts was performed as previously described (53). For gene deletion using CRISPR/Cas9 system, the mixture of sgRNA, the donor expression cassette, and the Cas9-expression cassette at a molar concentration ratio of 1:1:1 were cotransformed into the WT or mutant protoplasts. The putative transformants were screened using the corresponding antibiotics and then verified by PCR and DNA sequencing. The transformants carrying the fragments containing *bar* or *neo* were screened using phosphinothricin (100 μg/mL) or geneticin (80 μg/mL).

Transformation of *S. cerevisiae* was performed with the method as previously described (55) and then screened in SD medium lacking uracil to generate strains E(EGFP), E(*Mtcdt-2*), and E(*Mtcdt-2*-EGFP). The recombinant strains were identified by PCR and DNA sequencing.

The measure of cellulose and hemicellulose

To examine the utilization of cellulose and hemicellulose of corncob by *M. thermophila*, mature conidia were inoculated in 100 mL 1×VMM medium with 2% (w/v) corncob as carbon source. The cultures (25 mL) were harvested by filtering at different time-points and then washed with distilled water to obtain the total solids. For measuring the hemicellulose content, the solids were dried at 80 °C for 24 h, degraded in 1.5 mL 72% (w/w) H_2SO_4 at 30 °C for 1 h, after which 21.5 mL distilled water was added and the samples were incubated at 121 °C for 1 h. The final sample volume was adjusted to 25 mL. The xylose content in the acid hydrolysis

samples was measured using high-performance liquid chromatography (HPLC) and used for calculating hemicellulose content. The xylose in the mycelia was ignored because it was present at low levels. Before measuring the cellulose content, 15 mL acid hydrolysis solution (acetic acid:nitric acid:H_2O = 8:1:1) was added and the solution was vortexed and boiled for 1 h to eliminate mycelia and hemicellulose.

The solution was centrifuged and the precipitate was dried at 80 °C for 24 h. The dried samples were degraded as described above. The glucose content in the acid hydrolysis sample was measured for calculating cellulose content. The residual cellulose and hemicellulose contents (g/L) in the medium were calculated as follows: glucose content (g/L)/180.15 (g/mol) × (180.15 − 18.02) (g/mol); xylose content (g/L)/150.13 (g/mol) × (150.13 − 18.02) (g/mol).

Oligosaccharide assay

For the oligosaccharide analysis, 100 mL 1× VMM supplemented with different carbon sources, including 2% corncob, AX (1% Avicel and 1% xylan), 2% Avicel, and 2% xylan, was inoculated with *M. thermophila* (10^6 spores/mL). To prevent the release of soluble sugars due to heat, these carbon sources were not autoclaved. In addition, 100 μg/mL ampicillin was added to the medium to prevent bacterial contamination.

To prepare extracellular sugar samples, 5 mL cultures were centrifuged (4,000 rpm for 2 min at 4 °C). After adding 500 μL 50% methanol to a 1-mL aliquot of the supernatant, the solution was mixed thoroughly, placed on ice for 20 min and centrifuged (14,000 rpm for 30 min at 4 °C). The final supernatant was filtered through a 0.22 μm membrane and stored at −80 °C until assayed.

To prepare intracellular sugar samples, 5 mL cultures were centrifuged at 4 °C. The supernatant was discarded and the pellet was resuspended and washed three times with distilled water. Zirconium beads (0.5 mm) and 1 mL 50% methanol were added and the solution was mixed. The mixture was ground (15 times at 70 Hz for 70 s, with 30 s intervals) at −50 °C and then centrifuged (14,000 rpm for 30 min at 4 °C), filtered through a 0.22-μm membrane, and stored at −80 °C until assayed.

The oligosaccharides were analyzed using a Dionex CarboPac PA200 column (3 × 250 mm) and an ICS6000 high-performance anion exchange chromatography system equipped with a pulsed amperometric detector (HPAEC-PAD) with a gold working electrode and silver/silver chloride reference electrode (Thermo Fisher Scientific, Waltham, MA, USA). The column temperature was 30 °C, the injection volume was 10 μL, and the flow rate was 0.4 mL/min. The mobile phases were 100 mM NaOH and 1 M NaAc. The eluent gradient used for the analytical separation is listed in Dataset S9.

Enzymatic hydrolysis of hemicellulose and cellulose

Myceliophthora thermophila was cultured in 1× VMM supplemented with 2% Avicel, 2% xylan, or AX to induce the production of cellulases or hemicellulases. The protein concentration in the supernatant was determined using the Bio-Rad Protein Assay kit (absorbance of 595 nm) (Bio-Rad, Hercules, CA, USA). The hemicellulose/cellulose hydrolysis reaction system included the condensed culture (50 μg protein), 2% substrate (Avicel or xylan), and 1 μg/mL sodium azide in 1 mL 1× VMM. The samples were incubated at 45 °C for 24 h with shaking at 150 rpm and then centrifuged (14,000 rpm for 15 min at 4 °C). The supernatants were filtered through a 0.22 μm membrane and analyzed using an HPLC system.

Enzyme activity assay

For the assay of lignocellulolytic enzyme activities, *M. thermophila* strains were inoculated into 100 mL 1× VMM supplemented with 2% Avicel, 2% xylan, or AX. The BXL and BGL activities were measured on days 1 and 3, whereas XLN activity was measured on days 1 and 2. To measure extracellular enzyme activities, 1 mL cultures were centrifuged (14,000 rpm for 10 min at 4 °C) and the supernatant of each sample was retained. To measure intracellular enzyme activities, 100 mL cultures were passed through Whatman no. 1 filter paper to obtain mycelia, which were immediately frozen in liquid nitrogen. The frozen mycelia were ground to a powder in a prechilled mortar and dissolved in 20 mL precooled PBS buffer (137 mM NaCl, 2.7 mM KCl, 14.4 mM Na_2HPO_4, and 2.4 mM KH_2PO_4). The solution was thoroughly mixed and centrifuged at 4 °C for 10 min. The supernatant was collected for the enzyme activity assay. To protect proteins from proteases, phenyl methane sulfonyl fluoride (PMSF) was added to the samples (1 mM final concentration).

The protein concentration was determined using the Bio-Rad Protein Assay kit (absorbance of 595 nm). The BGL and BXL activity assays were completed using 4-nitrophenyl β-D-glucopyranoside (PNPG) and 4-nitrophenyl β-D-xylopyranoside (PNPX) as substrates, respectively. Before the assays, all reagents were preheated at 45 °C for 5 min and then 200 μL 1 mg/mL PNPG or PNPX was added to 200 μL supernatant, after which the solution was incubated at 45 °C for 10 min. The reaction was terminated by adding 500 μL 1 M Na_2CO_3. The mixtures were centrifuged (12,000 rpm for 3 min at 4 °C) and the absorbance (420 nm) of the supernatants was measured. To compare intracellular and extracellular BGL and BXL activities, the intracellular enzyme activity was calculated by dividing the total enzyme units in a 100 mL culture by the volume (i.e. 100 mL). To normalize the intracellular enzyme activity, the enzyme activity was calculated by dividing the total enzyme units by the corresponding protein content. One unit (U) of enzyme activity was defined as the amount of enzyme required to catalyze the formation of 1 μmol p-nitrophenol/min using PNPG or PNPX as the substrate at 45 °C and pH 4.8. The XLN activity assay was completed using the Azo-Xylan kit (Megazyme, Wicklow, Ireland).

Transcriptome analysis

Myceliophthora thermophila and its derivatives were cultured in 100 mL 1× VMM supplemented with 2% glucose at 45 °C for 18 h. Mycelia were harvested by filtering, washed three time with sterile water, and then transferred to fresh 1× VMM or 1× VMM supplemented with 2% Avicel, 2% xylan, AX (1% Avicel and 1% xylan), 2% glucose, 2% xylose, GX (1% glucose and 1% xylose), 0.5% cellobiose, 0.5% xylobiose, G2X2 (0.5% cellobiose and 0.5% xylobiose), GX2 (0.5% glucose and 0.5% xylobiose), or G2X (0.5% cellobiose and 0.5% xylose) as the carbon sources. After culturing for 4 h, total RNA was extracted as previously described (56) and sequenced using the Illumina HiSeq 2000 platform (Illumina, San Diego, CA, USA). Three biological replicates were analyzed for each culture condition. The data were processed and analyzed as previously described (57). The data of RNA-seq have been uploaded in Gene Expression Omnibus (accession number: GSE222371) at the National Center for Biotechnology Information.

Biomass measurement

The fungal biomass was measured on day 1 for samples grown on xylan and on day 3 for samples grown on Avicel. To measure the biomass of the fungi grown on xylan, mycelia were harvested and

washed three times with distilled water. After adding 1.5 mL 72% H_2SO_4 (w/w), the mycelial samples underwent degradation at 30 °C for 1 h, followed by the addition of distilled water and incubation at 121 °C for another hour. Subsequently, their volume was adjusted to 50 mL. The glucose content in the acid-hydrolyzed samples was measured using HPLC system. To calculate the biomass, a standard curve for the mycelial quantity and the glucose content after the acid hydrolysis was plotted in advance.

To measure the biomass of fungi grown on Avicel, 10 mL cultures were centrifuged to obtain a mixture of mycelia and residual Avicel. The mixture was washed twice with distilled water and dried at 80 °C to a constant weight (recorded as W0). The sample was hydrolyzed by adding 6 mL acid hydrolysis solution (acetic acid:nitric acid:H_2O; 8:1:1) and boiling in a water bath for 1 h, after which it was centrifuged. The precipitate was washed twice with distilled water and dried at 80 °C to a constant weight (recorded as W1). The difference between W0 and W1 was recorded as the mycelial weight in 10 mL cultures.

Residual sugar measurement

Myceliophthora thermophila and its derivatives were grown in 100 mL 1× VMM supplemented with 2% glucose as the carbon source. After an 18-h incubation at 45 °C, the mycelia were harvested by filtering and washed three times with distilled water. After starving the mycelia in 50 mL fresh 1× VMM for 30 min, 5 mL mycelia were added to a 24-well plate containing 0.5% glucose, 0.5% xylose, GX (0.5% glucose and 0.5% xylose), 0.5% cellobiose, 0.5% xylobiose, 0.5% xylotriose, G2X2 (0.5% cellobiose and 0.5% xylobiose), GX2 (0.5% glucose and 0.5% xylobiose), or GG2 (0.5% glucose and 0.5% cellobiose), and cultured at 45 °C with shaking at 700 rpm. To measure the residual sugar contents, 350-μL aliquots of the cultures were collected at different time-points. The samples were centrifuged and filtered through a 0.22 μm membrane prior to the HPLC analysis.

HPLC analysis

The sugar content was quantified using HPLC (e2695, Waters, Manchester, UK) equipped with a Waters 2414 refractive index detector. A high-performance carbohydrate column (4.6 × 250 mm) (Waters) and an Aminex HPX-87H column (Bio-Rad) were used for separating the oligosaccharides and monosaccharides, respectively. The oligosaccharides were detected at 35 °C using 70% acetonitrile as the mobile phase with a constant flow rate of 1 mL/min. The monosaccharides were detected at 45 °C using 5 mM H_2SO_4 as the mobile phase with a constant flow rate of 0.5 mL/min.

Confocal fluorescence microscopy

To localize the EGFP-tagged proteins, the recombinant *S. cerevisiae* strains E(EGFP) and E(*Mtcdt-2*-EGFP) were grown in SD medium at 30 °C on a rotary shaker (250 rpm) until the mid-exponential phase. The cells were centrifuged, spotted onto glass slides, and examined using a fluorescence microscope (Olympus BX51). Images were processed using Image J (58).

Oligosaccharide transport assay

Saccharomyces cerevisiae strains E(pRG426) and E(*Mtcdt-2*-EGFP) were grown in SD medium at 30 °C until the mid-exponential phase. Cells were harvested and washed three times with the transport buffer (5 mM MES and 100 mM NaCl; pH 6.0). The pellet was resuspended to a final OD_{600} of 60, after which a 500-μL aliquot of the resuspension was mixed with 500 μL sugar solution by vortexing. The following sugar substrates were used: 400 μM xylobiose, 400 μM cellobiose, 400 μM cellobiose, and 400 μM xylobiose (1:1), 800 μM cellobiose and 400 μM xylobiose (2:1), and 4,000 μM cellobiose and 400 μM xylobiose (10:1). When mixing, half of the volume was removed at the initial time-point (t = 0) and centrifuged to obtain the supernatant. The remaining solution was incubated for 30 min at 30 °C with shaking at 250 rpm and then centrifuged to collect the supernatant. For the HPAEC-PAD analysis, 0.5 M NaOH was added to the samples for a final concentration of 0.1 M. The sugar transport rate (%) was calculated as follows: (initial extracellular sugar content− residual extracellular sugar content at 0.5 h)/initial extracellular sugar content × 100.

Statistical analysis

Unless otherwise noted, statistical significance (ns, not significant; $^{*}P < 0.05$, $^{**}P < 0.01$, and $^{***}P < 0.001$) was assessed using a one-tailed homoscedastic (equal variance) t test. All *P*-values were generated using Microsoft Excel 2013 (Microsoft Corporation).

Acknowledgments

Many thanks to Prof. Eckhard Boles for generously sharing the strain *S. cerevisiae* EBY.VW4000.

Supplementary Material

Supplementary material is available at *PNAS Nexus* online.

Funding

This work was supported by funding from the Key Project of the Ministry of Science and Technology of China (2018YFA0900500), the Guangxi Science and Technology Major Program (Guike-AA22117013), the National Natural Science Foundation of China (31601013, 32071424, 2271481, and 32270100), the Tianjin Synthetic Biotechnology Innovation Capacity Improvement Project (TSBICIP-KJGG-015), and the Youth Innovation Promotion Association of the Chinese Academy of Sciences (2020183).

Author Contributions

J.Li and C.T. designed research. J.Liu, M.C., S.G., R.F., Z.Z., W.S., Y.Y., and J.Li performed research. J.Liu and J.Li contributed new reagents/analytic tools. J.Liu, M.C., J.Li, and C.T. analyzed data. J.Liu, J.Li, and C.T. wrote the paper.

Data Availability

All study data are included in the article and supplementary material.

References

1 Lu H, Yadav V, Bilal M, Iqbal HMN. 2022. Bioprospecting microbial hosts to valorize lignocellulose biomass—environmental perspectives and value-added bioproducts. *Chemosphere*. 288(Pt 2): 132574.

2 Broda M, Yelle DJ, Serwańska K. 2022. Bioethanol production from lignocellulosic biomass-challenges and solutions. *Molecules*. 27(24):8717.

3 Gírio FM, *et al.* 2010. Hemicelluloses for fuel ethanol: a review. *Bioresour Technol*. 101(13):4775–4800.
4 Zhong R, Cui D, Ye ZH. 2017. Regiospecific acetylation of xylan is mediated by a group of DUF231-containing O-acetyltransferases. *Plant Cell Physiol*. 58(12):2126–2138.
5 Sindhu R, Binod P, Pandey A. 2016. Biological pretreatment of lignocellulosic biomass—an overview. *Bioresour Technol*. 199: 76–82.
6 Gorke B, Stulke J. 2008. Carbon catabolite repression in bacteria: many ways to make the most out of nutrients. *Nat Rev Microbiol*. 6(8):613–624.
7 Gao M, Ploessl D, Shao Z. 2018. Enhancing the co-utilization of biomass-derived mixed sugars by yeasts. *Front Microbiol*. 9:3264.
8 Adnan M, *et al.* 2017. Carbon catabolite repression in filamentous fungi. *Int J Mol Sci*. 19(1):48.
9 Katahira S, *et al.* 2017. Screening and evolution of a novel protist xylose isomerase from the termite *Reticulitermes speratus* for efficient xylose fermentation in *Saccharomyces cerevisiae*. *Biotechnol Biofuels*. 10:203.
10 Kobayashi Y, Sahara T, Ohgiya S, Kamagata Y, Fujimori KE. 2018. Systematic optimization of gene expression of pentose phosphate pathway enhances ethanol production from a glucose/xylose mixed medium in a recombinant *Saccharomyces cerevisiae*. *AMB Express*. 8(1):139.
11 Wiedemann B, Boles E. 2008. Codon-optimized bacterial genes improve L-Arabinose fermentation in recombinant *Saccharomyces cerevisiae*. *Appl Environ Microbiol*. 74(7):2043–2050.
12 Kim SR, *et al.* 2013. Rational and evolutionary engineering approaches uncover a small set of genetic changes efficient for rapid xylose fermentation in *Saccharomyces cerevisiae*. *PLoS One*. 8(2): e57048.
13 Endalur Gopinarayanan V, Nair NU. 2018. A semi-synthetic regulon enables rapid growth of yeast on xylose. *Nat Commun*. 9(1): 1233.
14 Myers KS, *et al.* 2019. Rewired cellular signaling coordinates sugar and hypoxic responses for anaerobic xylose fermentation in yeast. *PLoS Genet*. 15(3):e1008037.
15 Wang M, Yu C, Zhao H. 2016. Directed evolution of xylose specific transporters to facilitate glucose-xylose co-utilization. *Biotechnol Bioeng*. 113(3):484–491.
16 Li H, Schmitz O, Alper HS. 2016. Enabling glucose/xylose co-transport in yeast through the directed evolution of a sugar transporter. *Appl Microbiol Biotechnol*. 100(23):10215–10223.
17 Lane S, *et al.* 2018. Glucose repression can be alleviated by reducing glucose phosphorylation rate in *Saccharomyces cerevisiae*. *Sci Rep*. 8(1):2613.
18 Hoang Nguyen Tran P, Ko JK, Gong G, Um Y, Lee SM. 2020. Improved simultaneous co-fermentation of glucose and xylose by *Saccharomyces cerevisiae* for efficient lignocellulosic biorefinery. *Biotechnol Biofuels*. 13:12.
19 Ha SJ, *et al.* 2011. Engineered *Saccharomyces cerevisiae* capable of simultaneous cellobiose and xylose fermentation. *Proc Natl Acad Sci U S A*. 108(2):504–509.
20 Olson DG, McBride JE, Shaw AJ, Lynd LR. 2012. Recent progress in consolidated bioprocessing. *Curr Opin Biotechnol*. 23(3):396–405.
21 Cragg SM, *et al.* 2015. Lignocellulose degradation mechanisms across the Tree of Life. *Curr Opin Chem Biol*. 29:108–119.
22 Wood TM. 1992. Fungal cellulases. *Biochem Soc Trans*. 20(1):46–53.
23 Andlar M, *et al.* 2018. Lignocellulose degradation: an overview of fungi and fungal enzymes involved in lignocellulose degradation. *Eng Life Sci*. 18(11):768–778.
24 Carle-Urioste JC, *et al.* 1997. Cellulase induction in *Trichoderma reesei* by cellulose requires its own basal expression. *J Biol Chem*. 272(15):10169–10174.
25 Delabona Pda S, Farinas CS, da Silva MR, Azzoni SF, Pradella JG. 2012. Use of a new *Trichoderma harzianum* strain isolated from the Amazon rainforest with pretreated sugar cane bagasse for on-site cellulase production. *Bioresour Technol*. 107:517–521.
26 Znameroski EA, *et al.* 2012. Induction of lignocellulose-degrading enzymes in *Neurospora crassa* by cellodextrins. *Proc Natl Acad Sci U S A*. 109(16):6012–6017.
27 Ilmen M, Saloheimo A, Onnela ML, Penttila ME. 1997. Regulation of cellulase gene expression in the filamentous fungus *Trichoderma reesei*. *Appl Environ Microbiol*. 63(4):1298–1306.
28 Aro N, Pakula T, Penttila M. 2005. Transcriptional regulation of plant cell wall degradation by filamentous fungi. *FEMS Microbiol Rev*. 29(4):719–739.
29 Wu VW, *et al.* 2020. The regulatory and transcriptional landscape associated with carbon utilization in a filamentous fungus. *Proc Natl Acad Sci U S A*. 117(11):6003–6013.
30 Berka RM, *et al.* 2011. Comparative genomic analysis of the thermophilic biomass-degrading fungi *Myceliophthora thermophila* and *Thielavia terrestris*. *Nat Biotechnol*. 29(10):922–927.
31 Jiang Y, Jiang W, Xin F, Zhang W, Jiang M. 2022. Thermophiles: potential chassis for lignocellulosic biorefinery. *Trends Biotechnol*. 40(6):643–646.
32 Huebner A, Ladisch MR, Tsao GT. 1978. Preparation of cellodextrins: an engineering approach. *Biotechnol Bioeng*. 20(10): 1669–1677.
33 Brown W, Anderson Ö. 1971. Preparation of xylodextrins and their separation by gel chromatography. *J Chromatogr A*. 57: 255–263.
34 Liu G, Qin Y, Li Z, Qu Y. 2013. Development of highly efficient, low-cost lignocellulolytic enzyme systems in the post-genomic era. *Biotechnol Adv*. 31(6):962–975.
35 Li J, *et al.* 2019. Dissecting cellobiose metabolic pathway and its application in biorefinery through consolidated bioprocessing in *Myceliophthora thermophila*. *Fungal Biol Biotechnol*. 6:21.
36 Znameroski EA, *et al.* 2014. Evidence for transceptor function of cellodextrin transporters in *Neurospora crassa*. *J Biol Chem*. 289(5):2610–2619.
37 Cai P, *et al.* 2014. Evidence of a critical role for cellodextrin transporte 2 (CDT-2) in both cellulose and hemicellulose degradation and utilization in *Neurospora crassa*. *PLoS One*. 9(2):e89330.
38 Lee WJ, Kim MD, Ryu YW, Bisson LF, Seo JH. 2002. Kinetic studies on glucose and xylose transport in *Saccharomyces cerevisiae*. *Appl Microbiol Biotechnol*. 60(1–2):186–191.
39 Hassan L, *et al.* 2019. Crosstalk of cellulose and mannan perception pathways leads to inhibition of cellulase production in several filamentous fungi. *mBio*. 10(4):e00277–e00219.
40 Li J, Lin L, Li H, Tian C, Ma Y. 2014. Transcriptional comparison of the filamentous fungus *Neurospora crassa* growing on three major monosaccharides D-glucose, D-xylose and L-arabinose. *Biotechnol Biofuels*. 7(1):31.
41 Zhang C, Acosta-Sampson L, Yu VY, Cate JHD. 2017. Screening of transporters to improve xylodextrin utilization in the yeast *Saccharomyces cerevisiae*. *PLoS One*. 12(9):e0184730.
42 Sternberg D, Mandels GR. 1979. Induction of cellulolytic enzymes in *Trichoderma reesei* by sophorose. *J Bacteriol*. 139(3): 761–769.
43 Chikamatsu G, Shirai K, Kato M, Kobayashi T, Tsukagoshi N. 1999. Structure and expression properties of the endo-beta-1,4-glucanase A gene from the filamentous fungus *Aspergillus nidulans*. *FEMS Microbiol Lett*. 175(2):239–245.

44 Suzuki H, Igarashi K, Samejima M. 2010. Cellotriose and cellotetraose as inducers of the genes encoding cellobiohydrolases in the basidiomycete *Phanerochaete chrysosporium*. *Appl Environ Microbiol*. 76(18):6164–6170.
45 Mandels M, Parrish FW, Reese ET. 1962. Sophorose as an inducer of cellulase in *Trichoderma viride*. *J Bacteriol*. 83(2):400–408.
46 Zhang P, *et al*. 2022. Induction of cellulase production in *Trichoderma reesei* by a glucose–sophorose mixture as an inducer prepared using stevioside. *RSC Adv*. 12(27):17392–17400.
47 Gielkens MM, Dekkers E, Visser J, de Graaff LH. 1999. Two cellobiohydrolase-encoding genes from *Aspergillus niger* require D-xylose and the xylanolytic transcriptional activator XlnR for their expression. *Appl Environ Microbiol*. 65(10):4340–4345.
48 Rolland F, Winderickx J, Thevelein JM. 2001. Glucose-sensing mechanisms in eukaryotic cells. *Trends Biochem Sci*. 26(5):310–317.
49 Ricci-Tam C, *et al*. 2021. Decoupling transcription factor expression and activity enables dimmer switch gene regulation. *Science*. 372(6539):292–295.
50 Lynd LR, Weimer PJ, van Zyl WH, Pretorius IS. 2002. Microbial cellulose utilization: fundamentals and biotechnology. *Microbiol Mol Biol Rev*. 66(3):506–577.
51 Parisutham V, Chandran SP, Mukhopadhyay A, Lee SK, Keasling JD. 2017. Intracellular cellobiose metabolism and its applications in lignocellulose-based biorefineries. *Bioresour Technol*. 239:496–506.
52 Wieczorke R, *et al*. 1999. Concurrent knock-out of at least 20 transporter genes is required to block uptake of hexoses in *Saccharomyces cerevisiae*. *FEBS Lett*. 464(3):123–128.
53 Liu Q, *et al*. 2017. Development of a genome-editing CRISPR/Cas9 system in thermophilic fungal *Myceliophthora* species and its application to hyper-cellulase production strain engineering. *Biotechnol Biofuels*. 10:1.
54 Xie S, Shen B, Zhang C, Huang X, Zhang Y. 2014. sgRNAcas9: a software package for designing CRISPR sgRNA and evaluating potential off-target cleavage sites. *PLoS One*. 9(6):e100448.
55 Gietz RD, Schiestl RH. 2007. High-efficiency yeast transformation using the LiAc/SS carrier DNA/PEG method. *Nat Protoc*. 2(1):31–34.
56 Xu G, *et al*. 2018. Transcriptional analysis of *Myceliophthora thermophila* on soluble starch and role of regulator AmyR on polysaccharide degradation. *Bioresour Technol*. 265:558–562.
57 Wang B, *et al*. 2017. Identification and characterization of the glucose dual-affinity transport system in *Neurospora crassa*: pleiotropic roles in nutrient transport, signaling, and carbon catabolite repression. *Biotechnol Biofuels*. 10:17.
58 Rueden CT, *et al*. 2017. Imagej2: imageJ for the next generation of scientific image data. *BMC Bioinformatics*. 18(1):529.